Long-term plasticity in interneurons of the dentate gyrus

Stephen T. Ross and Ivan Soltesz*

Department of Anatomy and Neurobiology, University of California, Irvine, CA 92697-1280

Edited by Per O. Andersen, University of Oslo, Norway, and approved May 4, 2001 (received for review January 26, 2001)

Single interneurons influence thousands of postsynaptic principal cells, and the control of interneuronal excitability is an important regulator of the computational properties of the hippocampus. However, the mechanisms underlying long-term alterations in the input–output functions of interneurons are not fully understood. We report a mechanism of interneuronal plasticity that leads to the functional enhancement of the gain of glutamatergic inputs in the absence of long-term potentiation of the excitatory synaptic currents. Interneurons in the dentate gyrus exhibit a characteristic, limited (≈8 mV) depolarization of their resting membrane potential after high-frequency stimulation of the perforant path. The depolarization can be observed with either whole-cell or perforated patch electrodes, and it lasts in excess of 3 h. The long-term depolarization is specific to interneurons, because granule cells do not show it. The depolarization requires the activation of Ca^{2+}-permeable α-amino-3-hydroxy-5-methyl-4-isoxazolepropionic acid (AMPA) receptors and the rise of intracellular Ca^{2+}, but not *N*-methyl-D-aspartate (NMDA) receptor activation. Data on the maintenance of the depolarization point to a major role for a long-term change in the rate of electrogenic Na^+/K^+-ATPase pump function in interneurons. As a result of the depolarization, interneurons after the tetanus respond with action potential discharges to previously subthreshold excitatory postsynaptic potentials (EPSPs), even though the EPSPs are not potentiated. These results demonstrate that the plastic nature of the interneuronal resting membrane potential underlies a unique form of long-term regulation of the gain of excitatory inputs to γ-aminobutyric acid (GABA)ergic neurons.

Hippocampal γ-aminobutyric acid (GABA)ergic interneurons regulate principal cell activity through a variety of mechanisms. Specialized interneuron classes have evolved to set the threshold for activation (1), shunt excitatory synaptic inputs (2, 3), prevent the backpropagation of fast action potentials in the dendrites (4, 5), inhibit dendritic Ca^{2+} electrogenesis (6), and synchronize sub- and suprathreshold membrane potential oscillations in spatially distributed principal cells (7–10). Because interneurons have powerful regulatory roles in the neuronal circuit, it is important to understand whether and how interneurons can undergo activity-dependent, long-term changes in their input–output functions. Recent data indicate that GABAergic synapses on hippocampal principal cells can be persistently modified, through both pre- and postsynaptic mechanisms (11–15). However, the activity-dependent regulation of excitatory synapses on interneurons is controversial and not thoroughly understood. Definitive demonstration of long-term potentiation (LTP) of monosynaptic excitatory inputs to interneurons is lacking, and recent data indicate that many types of hippocampal interneurons may be incapable of classical forms of LTP (16–19). In addition, high-frequency stimulation of excitatory afferents that evokes robust LTP in principal cells leads to either no change or long-term depression (LTD) in interneurons (20–23). Because interneurons differ from principal cells in many anatomical, neurochemical, and physiological properties, the gain of excitatory inputs to interneurons may be altered through mechanisms that are unexpected, and are distinct from the conventional LTP and LTD described for excitatory inputs to principal cells. A recent example of such a novel mechanism is the demonstration that interneurons in the CA1 stratum radiatum express a unique, heterosynaptic form of LTD (20).

We used tetanic stimulation of glutamatergic afferents to show that the resting membrane potential of dentate interneurons can effectively "remember" recent increases in excitatory activity. The mechanism described in this study can provide a means of setting the general excitability of interneurons as a function of the activity level of presynaptic principal cells, even in the absence of LTP of excitatory postsynaptic currents.

Methods

Slice Preparation. Horizontal brain slices (350 μm) were prepared from juvenile Wistar rats (15–22 days old) as described (24). The slices were incubated at 32°C in oxygenated (95% O_2/5% CO_2) artificial cerebrospinal fluid (ACSF) composed of 126 mM NaCl, 2.5 mM KCl, 26 mM $NaHCO_3$, 2 mM $CaCl_2$, 2 mM $MgCl_2$, 1.25 mM NaH_2PO_4, and 10 mM glucose, in a holding chamber for a minimum of 1 h before stimulation or recording.

Electrophysiology. Individual slices were transferred to a recording chamber perfused with oxygenated ACSF at 34°C, which, depending on the experiment, contained some of the following drugs: 1 μM tetrodotoxin (TTX) (Calbiochem), 10 μM 2-amino-5-phosphonovaleric acid (APV), 5 μM 6-cyano-7-nitroquinoxaline-2,3-dione (CNQX), 100 μM ZD-7288, 500 μM (*RS*)-α-methyl-4-carboxyphenylglycine (MCPG), 5 μM N-(4-hydroxyphenylpropanyl)spermine (NHPP-SP) (all from Tocris Neuramin, Bristol, U.K.), 10 μM bicuculline methiodide, or 30–100 μM strophanthidin (Sigma). All salts were obtained from Fluka. Patch pipettes, pulled from borosilicate (KG-33) glass capillary tubing (1.5 mm o.d.; Garner Glass, Claremont, CA) were filled with pipette solutions consisting of 140 mM potassium gluconate, 2 mM $MgCl_2$, and 10 mM Hepes. In some experiments the internal solution also included 20 mM sodium gluconate (replacing potassium gluconate), 10 mM EGTA and/or 4 mM ATP, or biocytin (0.3%), or 10–20 μg/ml gramicidin, or 200 μM sodium vanadate (Sigma) as specified in *Results*. Infrared-differential interference contrast microscopy-aided visualized techniques were used (Axioscope FS, Zeiss). Tetanic stimulation (5 trains of 10 s stimuli at 100 Hz, delivered at 30-s intervals, except in Fig. 1*E*) was carried out with a bipolar stimulating electrode placed in the perforant path, just above the hippocampal fissure, at the crest of the dentate gyrus. The stimulation intensity for the tetanus was 50% of firing threshold to low-frequency stimulation (0.1 Hz). Evoked exci-

This paper was submitted directly (Track II) to the PNAS office.

Abbreviations: LTP, long-term potentiation; LTD, long-term depression; ACSF, artificial cerebrospinal fluid; iLTDep, interneuronal long-term depolarization; V_m, resting membrane potential; TTX, tetrodotoxin; APV, 2-amino-5-phosphonovaleric acid; CNQX, 6-cyano-7-nitroquinoxaline-2,3-dione; MCPG, (*RS*)-α-methyl-4-carboxyphenylglycine; NHPP-SP *N*-(4-hydroxyphenylpropanyl)spermine; AMPA, α-amino-3-hydroxy-5-methyl-4-isoxazolepropionic acid; NMDA, *N*-methyl-D-aspartate; $GABA_A$ receptor, γ-aminobutyric acid type A receptor; R_N, input resistance; EPSP, excitatory postsynaptic potential.

*To whom reprint requests should be addressed. E-mail: isoltesz@uci.edu.

The publication costs of this article were defrayed in part by page charge payment. This article must therefore be hereby marked "*advertisement*" in accordance with 18 U.S.C. §1734 solely to indicate this fact.

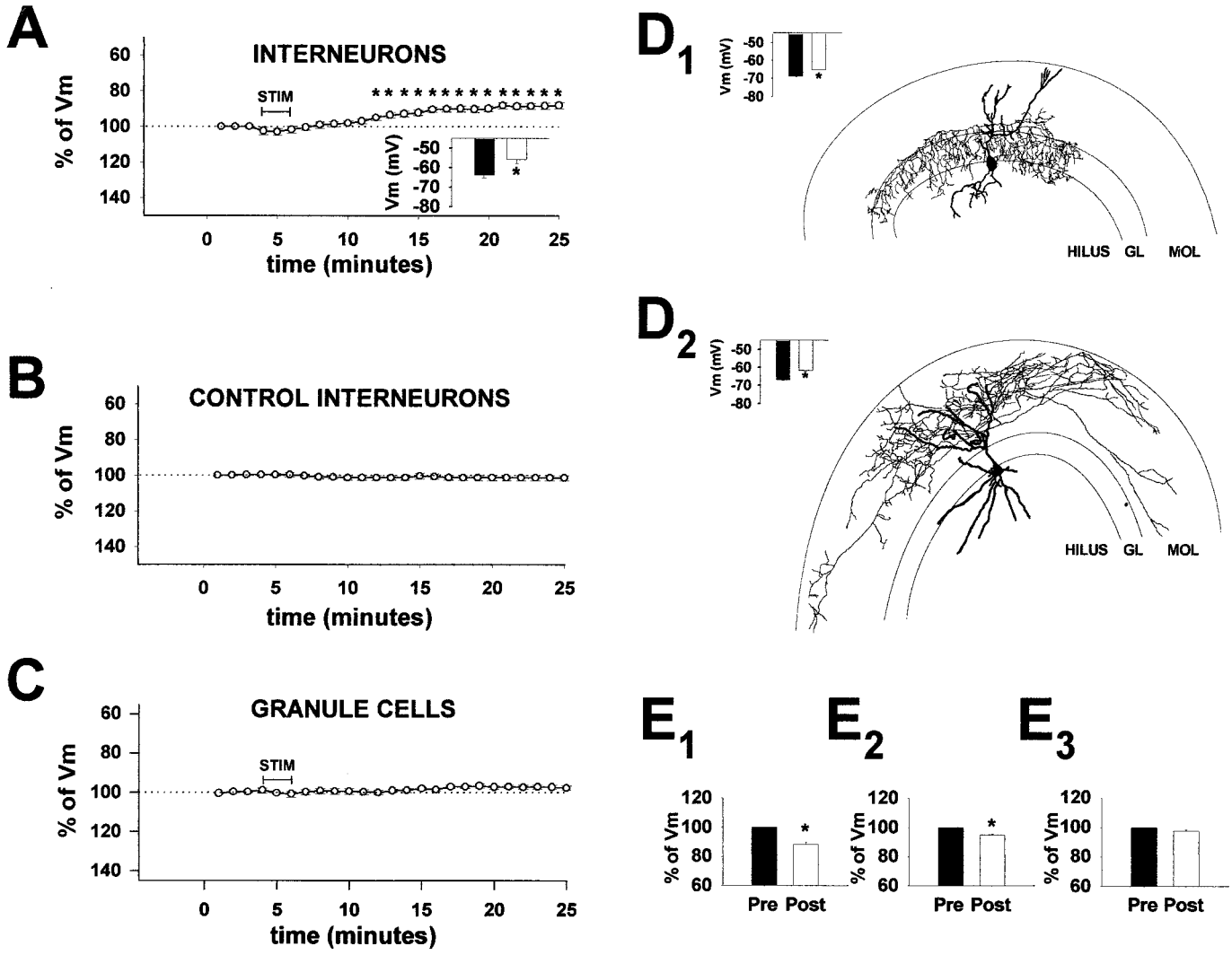

Fig. 1. Interneurons at the granule cell layer–hilar border, but not the granule cells, are persistently depolarized after tetanic stimulation of the perforant path. (*A*) Summary plot of the resting membrane potential (V_m) of interneurons ($n = 12$) as a function of recording time before and after tetanic stimulation of the perforant path (''STIM'': five 10-s trains at 100 Hz, delivered at 30-s intervals, used throughout this study, except in *E*), as percentage of prestimulation V_m (asterisks indicate significantly depolarized V_m). (*Inset*) Filled bar, V_m during the 3-min period before stimulation; open bar, V_m 20 min after stimulation. (*B*) Summary plot of interneuronal V_m ($n = 5$ cells) in the absence of stimulation. (*C*) Summary plot of V_m in granule cells ($n = 5$) before and after stimulation. (*D*) Camera lucida drawings of two interneurons that displayed iLTDep, with axonal projections limited primarily to the stratum granulosum (D_1) or to the stratum moleculare (D_2). (*Insets*) Filled bars, prestimulation V_m in each of the two illustrated cells; open bars, $V_{m20'}$ in each cell. (*E*) Summary of prestimulation V_m (''Pre'') and poststimulation $V_{m,20'}$ (''Post'') values of three tetanic stimulation paradigms: E_1, same as in *A*; E_2, three 1-s trains at 100 Hz, delivered at 10-s intervals, $n = 3$ (23); E_3, a single 1-s train at 100 Hz, $n = 3$.

tatory postsynaptic potentials (EPSPs; at 0.1 Hz; stimulus duration, 20 μs) were elicited with the stimulating electrode also used for the tetanus. Extracellular [K^+] measurements were made using individually calibrated valinomycin ion sensitive electrodes (25). For experiments involving biocytin labeling, the slices were fixed in 4% paraformaldehyde/0.5% glutaraldehyde, and reacted with 0.015% 3,3diaminobenzidine·tetrahydrochloride, and 0.006% H_2O_2. The slices were then cleared in ethanol, mounted, and reconstructed with a camera lucida.

Data Acquisition and Analysis. Recordings were obtained by using a NeuroData (Cygnus Instruments) or an Axopatch-200B (Axon Instruments) amplifier. Data were analyzed by using the STRATHCLYDE ELECTROPHYSIOLOGY software (courtesy of J. Dempster) and SYNAPSE software (courtesy of Y. De Koninck). For measurement of resting membrane potential (V_m), the recordings were sampled at 1 kHz for 20 s in each minute of recording, and the mean value of the membrane potential was calculated for each minute. For each cell, the V_m values during the 3 min before stimulation were averaged and taken as 100% (control period), and the poststimulation V_m data for each minute were expressed as a percentage of control V_m (e.g., Fig. 1*A*). Statistical analysis was performed using SIGMAPLOT with a level of significance of $P \leq 0.05$. Data are presented as means ± SE.

Results

Long-Term Depolarization of Dentate Interneurons. Tetanic stimulation of the perforant path resulted in three characteristic phases of V_m change in interneurons located at the granule cell layer–hilar border (Fig. 1*A*). The first phase took place during and immediately after stimulation. It was characterized by a hyperpolarization of V_m between stimulation epochs, likely related to activation of Ca^{2+}-activated K-conductances during

interneuronal firing triggered by the stimulation of afferent fibers. During the second phase, V_m temporarily appeared to return to control, prestimulation levels (Fig. 1*A*). However, during the third phase, the interneuronal V_m continued to shift toward the depolarizing direction, reaching a steady-state value ≈10 min after the end of the stimulation episode (Fig. 1*A*) (interneuronal V_m before stimulation: −63.6 ± 1.7 mV; V_m 20 min after stimulation ($V_{m,20'}$): −55.9 ± 1.9 mV; n = 12). When expressed in relative terms, $V_{m,20'}$ was 87.9 ± 1.7% of the prestimulation control level (100.0 ± 0.4%) (Fig. 1*A*). The tetanus-induced persistent depolarization was named interneuronal long-term depolarization (iLTDep).

When interneurons were recorded without stimulation, iLTDep did not take place (Fig. 1*B*) ($V_{m,20'}$ = 101.4 ± 1.4%; n = 5). Next, gramicidin perforated patch clamp experiments were performed. These experiments showed that iLTDep could also be observed with gramicidin perforated patch clamp recordings ($V_{m,20'}$ = 89.6 ± 1.3%; n = 4).

In contrast to interneurons, dentate granule cells did not change their V_m after stimulation ($V_{m,20'}$ = 97.7 ± 1.2%, n = 5; Fig. 1*C*). The iLTDep could be evoked in 100% of the interneurons tested, and morphological analysis of biocytin-filled interneurons showed that both interneurons with axons restricted to stratum granulosum (n = 3; Fig. 1D_1) and those with axons confined to stratum moleculare (n = 5; Fig. 1D_2) exhibited iLTDep in response to high-frequency stimulation of the perforant path. The tetanus did not alter the action potential adaptation properties of the interneurons (frequency of the last two versus the first two spikes in a train evoked by depolarizing current pulses from −60 mV: before tetanus: 0.83 ± 0.07; 20 min after tetanus: 0.85 ± 0.06). The iLTDep could be evoked with a less intense tetanic stimulation protocol (three 1-s trains at 10 s; n = 3) (23), but not when a single 1-s 100-Hz train was used (n = 3) (Fig. 1*E*).

To determine whether iLTDep lasts beyond the time limitation posed by recording from a single cell, tetanic stimulation of the perforant path was carried out in slices without recording from the interneurons during the stimulation. The stimulated and the similarly handled sham-stimulated (i.e., the stimulating electrode was placed in the perforant path, but no stimulation was applied) control slices were returned to a holding chamber, and whole-cell recordings were obtained from interneurons 1–4 h later. The V_m of interneurons in the stimulated slices were significantly more depolarized compared with controls (control: −67.4 ± 1.1 mV; tetanized: −61.0 ± 2.1 mV; n = 8 in both groups), indicating the iLTDep lasts for hours after its induction.

Additional experiments were carried out to determine whether the pattern of excitatory afferent stimulation was important in triggering iLTDep. Slices were incubated in 10 μM glutamate in ACSF for 3 min, followed by a wash in ACSF for 1–4 h. Control slices were handled similarly, but the incubation medium did not contain glutamate. Interneurons from slices exposed to glutamate showed a depolarized V_m compared with controls (control: −66.3 ± 1.0 mV; after glutamate: −57.6 ± 2.4 mV, n = 12 in both groups), indicating that the temporal pattern of glutamate release is not a major factor in evoking iLTDep. Granule cells did not show depolarized V_m after glutamate incubation (control: −78.0 ± 1.4 mV, n = 5; after glutamate: −78.5 ± 0.7 mV; n = 6).

Mechanism of Induction of iLTDep. Intracellularly injected depolarizing current pulses (duration: 10 s, repeated five times, at 30-s intervals; amplitude was set in each interneuron to be large enough to evoke intense firing), mimicking the tetanic stimulation-induced action potential discharges, did not lead to iLTDep ($V_{m,20'}$ = 99.1 ± 1.2%; n = 3) (Fig. 2*A*). The depolarizing current pulses failed to lead to iLTDep, even though the total number of action potentials evoked by the depolarizing current pulses (506.7 ± 26) was higher than the number of spikes observed during the tetanus in the experiments in Fig. 1E_2 (119.7 ± 38) that resulted in iLTDep. The iLTDep could be evoked after tetanic stimulation of the perforant path in the presence of the *N*-methyl-D-aspartate (NMDA) receptor antagonist APV (10 μM; $V_{m,20'}$ = 91.8 ± 2.0%, n = 5) (Fig. 2*B*). The iLTDep could be induced even in a higher concentration of APV (50 μM) ($V_{m,20'}$ = 92.1 ± 0.9%, n = 3). In contrast, the α-amino-3-hydroxy-5-methyl-4-isoxazolepropionic acid (AMPA)/kainate receptor antagonist CNQX (5 μM) was able to fully block the induction of iLTDep ($V_{m,20'}$ = 101.4 ± 1.0%, n = 5) (Fig. 2*C*). The polyamine antagonist of Ca^{2+}-permeable AMPA receptors NHPP-SP (22) (5 μM) also prevented iLTDep ($V_{m,20'}$ = 104.3 ± 1.0%, n = 4) (Fig. 2*D*). Furthermore, inclusion of the Ca^{2+}-chelator EGTA (10 mM) in the recording pipette blocked the induction of iLTDep ($V_{m,20'}$ = 102.9 ± 2.1%, n = 3) (Fig. 2*E*). In contrast, voltage clamping the interneurons at −60 mV during stimulation did not prevent iLTDep ($V_{m,20'}$ = 95.4 ± 0.6%, n = 3; but see *Discussion*) (Fig. 2*F*). The iLTDep could also be evoked in the presence of the γ-aminobutyric acid type A ($GABA_A$) receptor antagonist bicuculline (10 μM) ($V_{m,20'}$ = 94.2 ± 1.1%; n = 3). These data indicate that Ca^{2+}-permeable AMPA receptors on interneurons (22, 23, 26) play a major role in iLTDep induction.

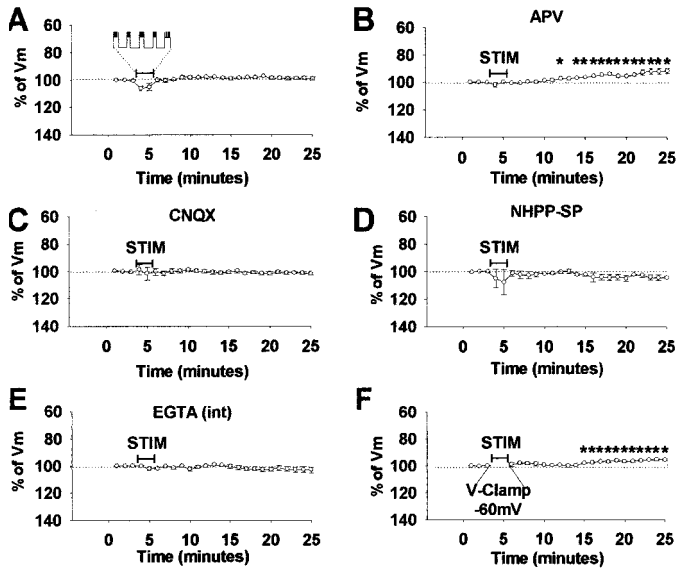

Fig. 2. Induction mechanisms of iLTDep. (*A*) Summary plot of V_m before and after intracellular current injection of depolarizing current pulses that strongly discharged the interneurons (n = 3), mimicking the depolarization and firing observed during the tetanic stimulation protocol. (*B–D*) Summary plots of iLTDep after perforant path stimulation in the presence of the NMDA receptor antagonist APV (*B*) (n = 5), and its block when the AMPA/kainate receptor antagonist CNQX (*C*) (n = 5), or the Ca^{2+}-permeable AMPA receptor antagonist NHPP-SP (*D*) (n = 4), was present in the perfusing medium. (*E*) Summary plot of the block of iLTDep by intracellular application of EGTA (n = 3). (*F*) Summary plot showing that iLTDep was not abolished when interneurons were voltage-clamped at −60 mV during stimulation (n = 3).

Mechanisms Underlying the Maintenance of iLTDep. iLTDep did not result in a significant change in input resistance (Fig. 3*B*). Input resistance measurements (R_N), measured using small hyperpolarizing pulses at −60 mV, during the prestimulation control period: 198.7 ± 36.5 MΩ; R_N during iLTDep, measured also at −60 mV, at the time point shown in Fig. 3*A*: 187.3 ± 31.5 MΩ;

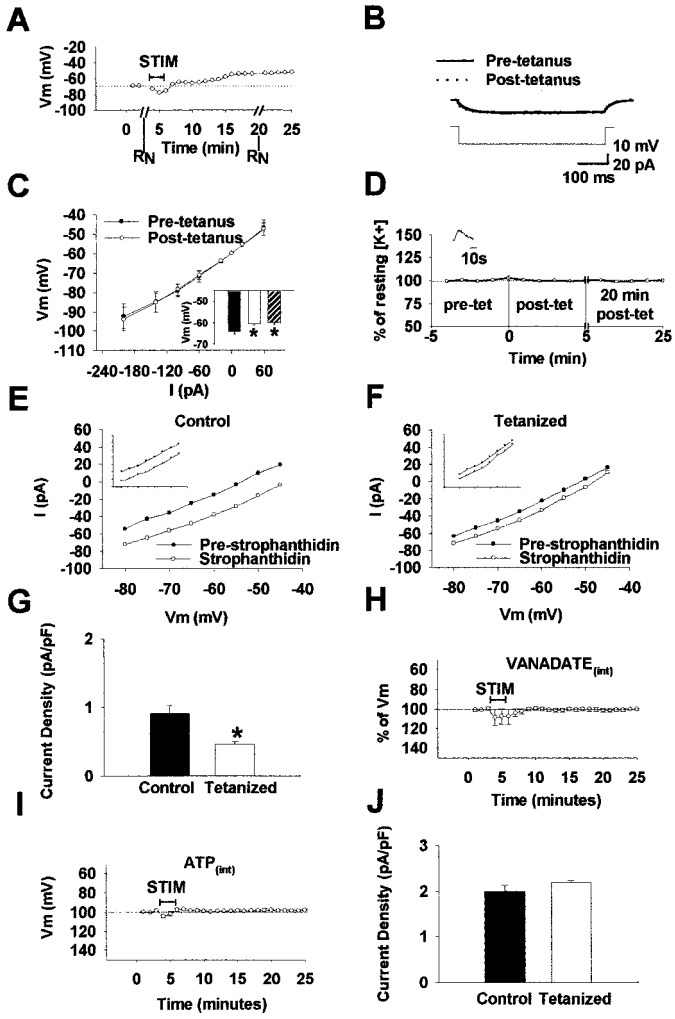

Fig. 3. Mechanisms underlying the maintenance of the iLTDep. (*A–C*) When current pulses were delivered before and after tetanic stimulation of the perforant path leading to iLTDep (*A*; time points of the input resistance measurements at −60 mV are indicated as "R_N"), no changes in R_N could be observed either with small (an example is shown in *B*) or larger current pulses (*C*). The plot of iLTDep in *A* and the traces in *B* are from the same interneuron. The summary plot in *C* is from $n = 6$ cells similar to that shown in *A* and *B*. The inset in *C* shows V_m values of interneurons before tetanus (filled bar), 20 min after tetanus (blank bar), and an additional 10 min after switching to ACSF containing APV, CNQX, MCPG, bicuculline, and TTX (hatched bar). (*D*) There was no sustained increase in extracellular K^+ after tetanic stimulation of the perforant path ($n = 3$ slices). (*Inset*) Tetanic stimulation evoked only transient changes in $[K^+]_o$. (*E–F*) I–V curves of interneurons from sham-stimulated (*E*) ($n = 4$ cells) and stimulated (*F*) ($n = 5$ cells) slices, before ("pre-strophanthidin") and in the presence of strophanthidin. The I–V curves were measured in APV, CNQX, bicuculline, TTX, and ZD-7288, in voltage clamp at zero current potential (note that strophanthidin caused a smaller shift in the I–V curve after tetanus at all membrane potentials). The *Insets* show examples of I-V curves from individual cells from sham-stimulated and stimulated slices, before and in the presence of strophanthidin. (*G*) Decreased pump current in interneurons from slices that were tetanized, compared with sham treated controls, from the experiments shown in *E–F*. (*H*) Summary plot ($n = 4$) showing that intracellular application of vanadate (a broad-spectrum blocker of phosphatases) abolished iLTDep. (*I*) Inclusion of ATP in the recording pipette also prevented the development of iLTDep ($n = 3$ cells; note that iLTDep could be evoked with gramicidin perforated patch recordings, as well as without recording from the interneurons during induction). (*J*) Pump current did not change when compounds that enhance pump rate (Na^+, ATP, and EGTA) were included in the pipette ($n = 3$ interneurons in both control and tetanized slices).

$n = 6$). As illustrated in Fig. 3*C*, larger current pulses also failed to detect a significant change in R_N in the same cells.

Next, the effect of blockade of NMDA, AMPA/Kainate, metabotropic glutamate, and $GABA_A$ receptors and Na^+ channels on iLTDep was tested. Twenty minutes after the induction of iLTDep, the perfusing solution was switched to ACSF containing 10 μM APV, 5 μM CNQX, 500 μM MCPG, 10 μM bicuculline, and 1 μM TTX, for 10 min. These drugs failed to reverse iLTDep; in fact, they induced a nonsignificant, additional 1.3 ± 1.4% depolarization in the $V_{m,20'}$ measured before the application of these antagonists (Fig. 3*C inset*).

In subsequent experiments, the extracellular $[K^+]$ was measured by using K^+-sensitive electrodes (25) before, during, and after tetanic stimulation. However, no sustained increases in $[K^+]_o$ could be observed in the granule cell layer (Fig. 3*D*; $n = 3$), and the K^+-transients evoked by the tetanic stimulation were cleared within 30 s (Fig. 3*D inset*).

The V_m of dentate interneurons is influenced by the activity of the electrogenic Na^+/K^+-ATPase (24). The interneuronal Na^+/K^+-ATPase activity (the pump current) was measured using brief (20-s) application of the pump blocker strophanthidin (30 μM) in interneurons from stimulated and sham-stimulated control slices. Pump blockade caused a smaller shift in the I–V curves at all membrane potentials in cells from stimulated slices (Fig. 3 *E* and *F*), indicating a significant reduction in the pump current density in interneurons expressing iLTDep (Fig. 3*G*) (control: 0.91 ± 0.12 pA/pF, $n = 5$; tetanized: 0.46 ± 0.04 pA/pF, $n = 4$). Note that these experiments were performed in the presence of APV, CNQX, bicuculline, TTX, and the hyperpolarization-activated cation channel (h-channel) blocker (100 μM ZD-7288), and the V_m in interneurons from stimulated slices was 81.4 ± 5.1% of V_m in cells from control slices. Because iLTDep could be observed in the presence of ZD-7288, these data also indicate that increased h-channel activity cannot underlie iLTDep. Next, the pump was blocked from the inside in the recorded interneuron by the inclusion of 200 μM vanadate, a broad-spectrum blocker of phosphatases known to inhibit the Na^+/K^+-ATPase (27), in the pipette-filling solution. iLTDep could not be observed with intracellular vanadate present (Fig. 3*H*) ($V_{m,20'} = 100.5 \pm 1.0\%$, $n = 4$). Inclusion of 4 mM ATP in the pipette solution also blocked iLTDep (Fig. 3*I*) ($V_{m,20'} = 98.3 \pm 1.02\%$, $n = 3$). Taken together, these data are consistent with a major role for the Na^+/K^+-ATPase in iLTDep.

Next, in interneurons from tetanized and control slices, the pump rate was enhanced with intracellular application of pump substrates (20 mM Na^+, 4 mM ATP) and a Ca^{2+}-chelator (10 mM EGTA, introduced to prevent the inhibition of the Na^+/K^+-ATPase by intracellular Ca^{2+}) (28, 29), followed by pump blockade with prolonged (5-min) application of 100 μM strophanthidin (24, 30, 31). Under these conditions, no difference in pump current density could be observed in interneurons from tetanized and sham-stimulated control slices (control: 1.99 ± 0.12 pA/pF, $n = 3$; tetanized: 2.18 ± 0.04 pA/pF, $n = 3$; Fig. 3*J*). Therefore, the decreased pump function was not caused by a decrease in the number of functionally available pump molecules in the membrane.

Enhanced Excitatory Gain in Interneurons as a Result of iLTDep. A series of "artificial EPSPs" (10-ms current pulses of 20- to 400-pA amplitude, at 1.0 Hz, in current clamp) were injected into interneurons before and during iLTDep (Fig. 4*A*). As expected, iLTDep caused a leftward shift in the input–output curve of interneurons (Fig. 4*B*; $n = 3$), indicating that previously subthreshold depolarizations can evoke action potential discharges after the induction of iLTDep. Similar results could be obtained by using "real" EPSPs (evoked by stimulation of the perforant path, with the stimulating electrode also used to evoke tetanic stimulation) (Fig. 4 *C* and *D*; $n = 4$). Control recordings in

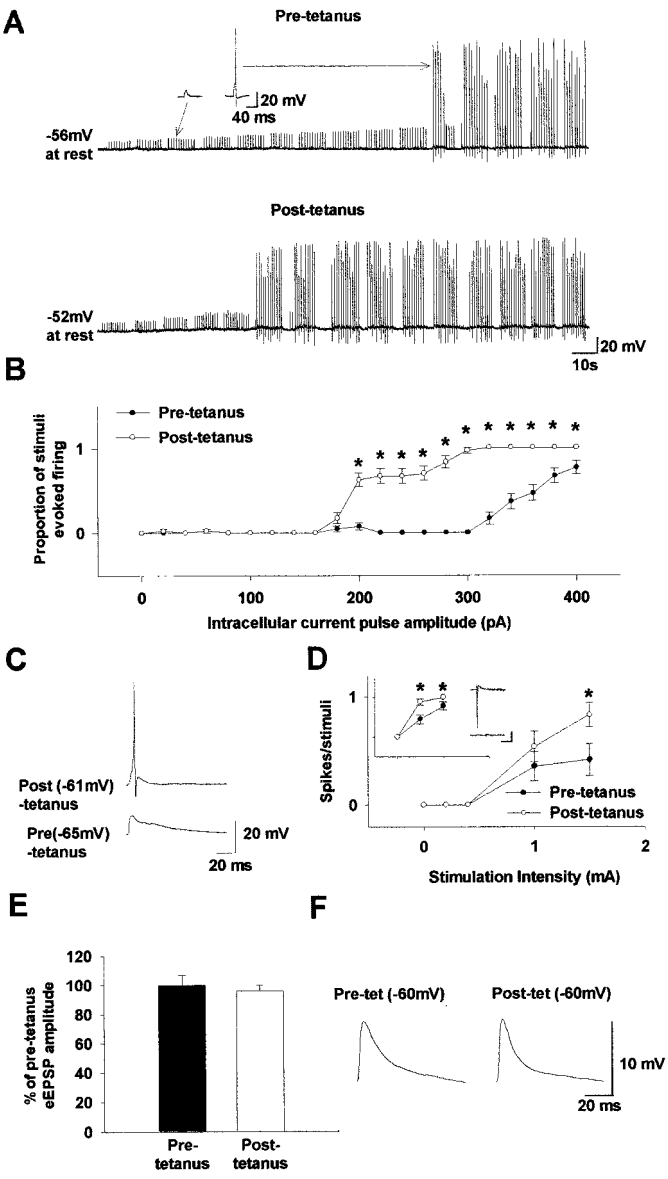

Fig. 4. iLTDep enhances the efficacy of EPSPs to fire the interneuron, even in the absence of LTP. (*A*) Voltage responses to a series of brief intracellular current pulses of increasing amplitude (10 ms; 20–400 pA) are shown in an interneuron before and after tetanic stimulation of the perforant path (*Insets*, subthreshold and suprathreshold EPSPs). (*B*) Summary plot ($n = 3$ cells, similar to the one shown in *A* of injected current versus action potential discharges before and 20 min after tetanic stimulation. (*C*) Evoked EPSPs recorded from an interneuron before and 20 min after tetanic stimulation, at the respective resting membrane potentials (stimulation intensity used to evoke the EPSPs: 1.5 mA in both cases). (*D*) Summary plot ($n = 4$ interneurons, from experiments similar to the one in *C*) of stimulation intensity to evoke EPSPs versus the proportion of stimuli that elicited action potential discharges. (*Inset*) Summary plot of stimulation intensity versus spikes/stimuli data from cell-attached recordings from interneurons ($n = 3$); *x*- and *y*-axes are as in *D*; representative traces are shown before (*Lower*) and after (*Upper*) tetanus; scale in *Inset*: 5 ms, 5 pA. (*E* and *F*) Tetanic stimulation of the perforant path did not alter the evoked EPSP (eEPSP) amplitude in interneurons, when measured at −60 mV before and during iLTDep (the traces in *F* are from an average of 30 responses).

cell-attached patch clamp mode also revealed a significantly enhanced interneuronal firing after tetanus (Fig. 4*D Inset*; $n = 3$). The enhanced firing after tetanic stimulation was due to iLTDep, because tetanic stimulation in these interneurons did not lead to LTP of the evoked EPSPs (Fig. 4 *E* and *F*), in agreement with data indicating that most hippocampal interneurons do not express LTP of their excitatory inputs (19).

Discussion

Interneuron-Specific Forms of Plasticity. The data in this paper show that dentate interneurons exhibit a form of synaptically induced long-term alteration that enhances the ability of excitatory inputs to reach firing threshold. LTP and LTD have mainly been studied in principal cells, and they are less understood in interneurons. A series of recent studies (17, 20, 22, 23) have reported either no change, or LTD in various hippocampal interneurons after tetanic stimulation. In agreement with studies on interneurons in Ammon's horn, dentate interneurons also failed to express LTP after tetanus (in fact, they showed a nonsignificant, 4.5% decrease in EPSP amplitude; Fig. 4*E*). Based on our data, it is likely that the presence of ATP and/or EGTA in the intracellular pipette solution used in most previous investigations precluded the development of iLTDep after tetanus. Interestingly, both the unusual form of interneuronal LTD found by McMahon and Kauer (20) and the iLTDep described in this study were dependent on the activation of Ca^{2+}-permeable, GluR2 subunit-lacking AMPA receptors expressed by interneurons (22, 23, 26). Therefore, the expression of Ca^{2+}-permeable AMPA receptors seems to play a central role in enabling interneurons to display various interneuron-specific forms of neuronal plasticity that are not exhibited by principal cells.

The iLTDep could be induced by two stronger tetanic stimulation paradigms (five 10-s trains at 100 Hz and three 1-s trains at 100 Hz), but not with one 1-s train at 100 Hz (Fig. 1*E*). These results suggest that iLTDep is likely to occur especially under conditions when extracellular glutamate is strongly increased, e.g., after seizure activity *in vivo*. Because incubation of the slices in glutamate was just as effective in inducing iLTDep as patterned tetanic stimulation, it is likely that the induction of this form of plasticity depends more on the overall activity levels in incoming excitatory afferents than on the specific temporal characteristics of inputs. Therefore, iLTDep may be thought of as a mechanism by which interneurons can adjust the gain of their excitatory inputs as a function of the level of action potential discharges in the presynaptic glutamatergic cells.

Role for Ca^{2+}-Permeable AMPA Receptors and Intracellular Ca^{2+} Rise. Our data show that Ca^{2+}-permeable AMPA receptor activation was necessary for the induction of iLTDep. The role of Ca^{2+} in the induction pathway was indicated by the ability of intracellular Ca^{2+}-chelation to block iLTDep. Possible roles for alternative (i.e., not related to Ca^{2+}-permeable AMPA receptors) pathways for Ca^{2+} entry were also examined. A major role for voltage-gated Ca^{2+} channels is unlikely, because depolarization and firing of interneurons by intracellular current pulses did not evoke iLTDep, and voltage-clamping the cells near rest did not fully block iLTDep. It should be noted that voltage-clamping the cells during induction did appear to cause a decrease in the development of iLTDep, but the decrease was nonsignificant (i.e., the $V_{m20'}$ values of the interneurons in current clamp in Fig. 1*A* and in voltage clamp in Fig. 2*F* were not statistically different). Therefore, it cannot be excluded that voltage-gated Ca^{2+} channels play a minor role in iLTDep. NMDA receptor blockade did not abolish iLTDep, indicating that Ca^{2+} entry through NMDA receptors is not required for the induction of this plasticity. In summary, these two alternative pathways for Ca^{2+} entry play either no or only a minor role in iLTDep induction.

It should also be noted that iLTDep did not occur when interneurons were recorded in the absence of tetanic stimulation (Fig. 1*B*). Furthermore, a shift in V_m after tetanic stimulation

was also observed with gramicidin perforated patch clamp recordings, in which there is minimal disturbance of the intracellular constituents of the recorded cells. These data, together with results showing that iLTDep could be observed in interneurons that were not even recorded during tetanic stimulation, indicate that iLTDep is not due to washout of intracellular constituents during whole-cell patch clamp recordings.

Maintenance of iLTDep. Once iLTDep was induced, antagonists of ionotropic and metabotropic glutamate receptors, $GABA_A$ receptors, voltage-gated Na^+ channels, and h-channels could not reverse it. Furthermore, there was no sustained extracellular rise in $[K^+]$, which was also indicated by the lack of LTD in granule cells (however, highly localized $[K^+]_o$ increases in the extracellular space immediately surrounding the interneurons cannot be excluded). Interneurons did not appear to change their input resistance significantly during iLTDep, tested either with small negative and positive current pulses, or with large negative pulses spanning over 40 mV. These latter results suggest that iLTDep is unlikely to be explained by the closure of voltage-dependent or independent K channels. It has been shown that extracellular Cs^+ (in the presence of the h-channel blocker ZD-7288) has no effect on the inward current below the reversal potential for potassium ions (E_K) in interneurons in the dentate granule cell layer, suggesting low levels of expression of the classical anomalous K^+-dependent inward rectifier in these cells (24). Nevertheless, a small net contribution from K channels to iLTDep cannot be excluded.

In contrast, the electrogenic Na^+/K^+-ATPase pump current, which generates a steady-state hyperpolarizing influence in dentate interneurons (24), was significantly decreased after tetanic stimulation. Taken together, the lack of a detectable change in R_N, the decreased pump current measured by using the Na^+/K^+-ATPase blocker strophanthidin, the abolishment of iLTDep by intracellular vanadate, and the block of iLTDep by intracellular ATP, are all consistent with, and point to, the Na^+/K^+-ATPase pump as a major mechanism underlying iLTDep in interneurons. The present study supports data from other reports indicating that the Na^+/K^+-ATPase can be modulated by glutamate receptor-dependent mechanisms (28–31). It has been shown that the strophanthidin-sensitive current amplitude is in the same order of magnitude in granule cells and interneurons (24), indicating that the differential activity-dependent modulation of the V_m of granule cells and interneurons is unlikely to be related to the baseline pump rate. Modulation of Na^+/K^+-ATPase function on the time scale of minutes and hours is known to occur as a result of intracellular Ca^{2+} rises, decreased intracellular ATP levels, and phosphorylation, whereas longer-term modulation involves translocation of the pump molecules from the membrane to the intracellular compartment (24, 28–33). Whether the decreased pump current in the present study is due to a change in Na^+/K^+-ATPase subunit composition (32, 33), altered phosphorylation status (33), or a sustained drop in intracellular ATP levels (30) will need to be decided by future experiments. However, our results, which show that the pump current remains unchanged by tetanic stimulation after the pump rate is enhanced by the intracellular application of pump substrates and EGTA, indicate that the number of pump molecules is not altered by translocation during iLTDep.

Conclusions

In summary, these data provide evidence for a previously undescribed mechanism by which interneurons can modulate the efficacy of their excitatory inputs, depending on the levels of activity in the presynaptic glutamatergic pathway. The results show that the resting membrane potential can be persistently modulated in interneurons, allowing the long-term enhancement of the functional gain of depolarizing inputs to interneurons even in the absence of conventional LTP of the incoming excitatory synaptic events.

We thank Drs. K. Kaila and J. Voipio for help with the $[K^+]_o$-measurement techniques, and Ms. R. Zhu for technical assistance. This study was supported by National Institutes of Health Grant NS 35915 (to I.S.).

1. Andersen, P., Eccles, J. C. & Loyning, Y. (1963) *Nature (London)* **198,** 540–542.
2. Qian, N. & Sejnowski, T. J. (1990) *Proc. Natl. Acad. Sci. USA* **87,** 8145–8149.
3. Staley, K. J. & Mody, I. (1992) *J. Neurophysiol.* **68,** 197–212.
4. Buzsáki, G., Penttonen, M., Nadasdy, Z. & Bragin, A. (1996) *Proc. Natl. Acad. Sci. USA* **93,** 9921–9925.
5. Tsubokawa, H. & Ross, W. N. (1996) *J. Neurophysiol.* **76,** 2896–2906.
6. Miles, R., Toth, K., Gulyas, A. I., Hajos, N. & Freund, T. F. (1996) *Neuron* **16,** 815–823.
7. Soltesz, I. & Deschênes, M. (1993) *J. Neurophysiol.* **70,** 97–116.
8. Ylinen, A., Soltesz, I., Bragin, A., Pentonnen, M., Sik, A. & Buzsáki, G. (1995) *Hippocampus* **5,** 78–91.
9. Cobb, S. R., Buhl, E. H., Halasy, K., Paulsen, O. & Somogyi, P. (1995) *Nature (London)* **378,** 75–78.
10. Whittington, M. A., Traub, R. D. & Jefferys, J. G. R. (1995) *Nature (London)* **373,** 612–615.
11. Otis, T. S., De Koninck, Y. & Mody, I. (1994) *Proc. Natl. Acad. Sci. USA* **91,** 7698–7702.
12. Nusser, Z., Hájos, N., Somogyi, P. & Mody, I. (1998) *Nature (London)* **395,** 172–177.
13. Brooks-Kayal., A.R., Shumate, M. D., Jin, H., Rikhter, T. Y. & Coulter, D. A. (1998) *Nat. Med.* **4,** 1166–1172.
14. Buhl, E. H., Otis, T. S. & Mody, I. (1996) *Science* **271,** 369–373.
15. Chen, K., Baram, T. Z. & Soltesz, I. (1999) *Nat. Med.* **5,** 888–894.
16. Ouardouz, M. & Lacaille, J. C. (1995) *J. Neurophysiol.* **73,** 810–819.
17. Maccaferri, G. & McBain, C. J. (1995) *Neuron* **15,** 137–145.
18. Maccaferri, G. & McBain, C. J. (1996) *J. Neurosci.* **16,** 334–343.
19. McBain, C. J., Freund, T. F. & Mody, I. (1999) *Trends Neurosci.* **22,** 228–235.
20. McMahon, L. L. & Kauer, J. A. (1997) *Neuron* **18,** 295–305.
21. Maccaferri, G., Tóth, K. & McBain, C. J. (1998) *Science* **279,** 1368–1370.
22. Laezza, F., Doherty, J. J. & Dingledine, R. (1999) *Science* **285,** 1411–1414.
23. Toth, K., Suares, G., Lawrence, J. J., Philips-Tansey, E. & McBain, C. (2000) *J. Neurosci.* **20,** 8279–8289.
24. Ross, S. T. & Soltesz, I. (2000) *J. Neurophysiol.* **83,** 2916–2930.
25. Voipio, J., Pasternack, M. & Macleod, K. (1994) *Microelectrode Techniques*, ed. Ogden, D. (Company of Biologists, Cambridge, U.K.), pp. 276–316.
26. Tóth, K. & McBain, C. J. (1998) *Nat. Neurosci.* **1,** 572–578.
27. Benham, C. D., Evans, M. L. & McBain, C. J. (1992) *J. Physiol. (London)* **455,** 567–583.
28. Fukuda, A. & Prince, D. A. (1992) *J. Neurophysiol.* **68,** 28–35.
29. Lees, G. J. (1991) *Brain Res. Rev.* **16,** 283–300.
30. Tavalin, S. J., Ellis, E. F. & Satin, L. S. (1997) *J. Neurophysiol.* **77,** 632–638.
31. Gadsby, D. C. & Nakao, M. (1989) *J. Gen. Physiol.* **94,** 511–537.
32. Inoue, N., Soga, T. & Kato, T. (1999) *NeuroReport* **10,** 3289–3293.
33. McDonough, A. A. & Farley, R. A. (1993) *Curr. Opin. Nephrol. Hypertens.* **2,** 725–734.